



ELSEVIER

Available online at www.sciencedirect.com

SCIENCE @ DIRECT®

Journal of Sound and Vibration 287 (2005) 277–295

JOURNAL OF
SOUND AND
VIBRATION

www.elsevier.com/locate/jsvi

Vibration of beams with multiple open cracks subjected to axial force

Baris Binici*

Department of Civil Engineering, Middle East Technical University, İnönü Bulvarı 06531, Ankara, Turkey

Received 15 April 2004; received in revised form 28 October 2004; accepted 3 November 2004

Available online 28 January 2005

Abstract

A new method is proposed to obtain the eigenfrequencies and mode shapes of beams containing multiple cracks and subjected to axial force. Cracks are assumed to introduce local flexibility changes and are modeled as rotational springs. The method uses one set of end conditions as initial parameters for determining the mode shape functions. Satisfying the continuity and jump conditions at crack locations, mode shape functions of the remaining parts are determined. Other set of boundary conditions yields a second-order determinant that needs to be solved for its roots. As the static case is approached, the roots of the characteristic equation give the buckling load of the structure. The proposed method is compared against the results predicted by finite element analysis. Good agreement is observed between the proposed approach and finite element results. A parametric study is conducted in order to investigate the effect of cracks and axial force levels on the eigenfrequencies. Both simply supported and cantilever beam-columns are considered. It is found that eigenfrequencies are strongly affected by crack locations, severities and axial force levels. Simple modifications to account for flexible intermediate supports are presented as well. The proposed method can efficiently be used in detecting crack locations, severities and axial forces in beam-columns. Furthermore it can be used to predict the critical load of damaged structures based on eigenfrequency measurements.

© 2004 Elsevier Ltd. All rights reserved.

*Tel.: +90 312 210 2457; fax: +90 312 210 1193.

E-mail address: binici@metu.edu.tr (B. Binici).

1. Introduction

Deteriorating infrastructure has resulted in a surge of techniques for identification of damage in structural elements. Use of eigenfrequency changes in damaged structural elements has been widely investigated for their possible use in damage detection studies [1,2]. The ease of experimentation and data processing associated with frequency-based detection schemes make them attractive from an engineering perspective. However, consideration of all factors that can influence vibration frequencies is required to accurately detect cracks. For structural elements that are subjected to axial loads, such as building columns and bridge piers, the effect of axial force on eigenfrequencies can be significant. Furthermore, determining axial loads from vibration data is a method used for capacity evaluation of columns. These factors require axial forces to be considered in vibration analyses. In order to solve the inverse problems (i.e. detection of crack locations and severity) associated with these structural elements, efficient forward problem solution techniques are required.

Vibrations of cracked structures have been widely investigated in the last three decades. Several approaches for determining natural frequency changes due to presence of a single crack have been studied [3–5]. For the case of multiple cracks, a number of approaches were proposed to determine the eigenfrequencies [6,7]. The improved analytical formulation by Li [7,8] makes use of the boundary conditions and recursive formulas to reduce the problem to finding the roots of the second-order determinant. Arbitrary numbers of cracks and concentrated masses can be handled easily with the method proposed by Li [7]. In these solutions, effects of axial forces were not considered. Krawczuk and Ostachowicz [9] employed finite element analysis in order to determine eigenfrequencies by taking into account the effect of axial force through the use of the geometric stiffness matrix. Their study was limited to structures containing a single crack. The inverse problem, i.e. finding the location and severity of cracks from frequency measurements, has been investigated using the finite element method [10,11], the transfer matrix approach [12] and perturbation solutions [13]. State of the art review studies have been presented on damage identification procedures [1,2,14].

Other studies have been conducted on stability of cracked and uncracked structures [15–18]. Chen and Chen [15] investigated the stability of a rotating shaft with a single crack. Their study examined the dynamic stability of the shaft under the assumptions of Timoshenko beam theory. Li [16] used a transfer matrix approach to determine buckling loads of multi-stepped beam-columns. Naguleswaran [17] examined the stability and vibration of an undamaged beam-column up to three step changes. Takahashi [18] used a transfer matrix approach for vibration and stability analysis of a non-uniform shaft with a single crack. Vibration and stability of a cracked translating beam has been investigated by Murphy and Zhang [19]. In these studies [16,18,19] cracks were assumed to remain open regardless of the modes and cycle of vibration. Murphy and Zhang [19] studied the static bending moment and axial force resulting in an “open crack” condition for a simply supported beam. They concluded that a tensile load together with a positive bending moment results in an open crack whereas a compressive load and a negative bending moment results in a closed crack. For cases that signs of the axial load and bending moment are opposite, these researchers found a linear relationship between the axial force and bending moment for which crack remains open [19]. Such a criterion for cracks present on axially loaded vibrating beams depends on the axial load level, amplitude of the excitation, the locations

of the cracks and eigenmode under consideration. Furthermore, resulting problem is nonlinear due to change in local flexibility during crack closure, and the use of time domain analysis is necessary. Instead, current study primarily focuses on the proposed method of solution in the frequency domain, where all cracks are assumed to remain open. This assumption is believed to represent a limiting condition for the flexibilities introduced due to the presence of cracks.

Plane of buckling depends on the direction about which moment of inertia of the cross section is minimum [20]. When buckling occurs in a plane parallel to the crack direction (out of plane), part of the crack can close while part of it remains open, resulting in a nonlinear problem. Conversely, when buckling plane is perpendicular to the crack direction (in plane), it is realistic to assume that cracks are open in the deformed configuration [16]. This study refers to the latter case of in-plane buckling where crack directions are assumed to be parallel to the shorter side of a rectangular cross section. In this way, buckling plane is ensured to be perpendicular to the crack directions for which open crack assumption is reasonable. Moreover, for cracks developed under service loads, it is not unrealistic to expect crack directions be perpendicular to the weakest plane of axis about which buckling can occur.

Apart from approaches for determining vibration and stability behavior of beam-columns with the use of numerical methods [10,12] and classical solutions for cases without any cracks [20,21], closed form solutions are required for damaged beam-columns subjected to axial force. The objective of this study is to introduce a new method to determine natural frequencies and mode shapes of beam-columns containing multiple cracks. The mode shape functions are expressed in terms of initial parameters that satisfy the boundary conditions. The approach results in a second-order determinant with the consideration of axial force. As the static case is approached, it also gives the critical load for the structure considered. Parametric studies are conducted to investigate the effects of axial force, crack locations and severities on the eigenfrequency changes for beam-columns with boundary conditions that are commonly encountered in engineering practice.

2. Theoretical development

An Euler–Bernoulli beam containing multiple cracks with a constant axial force is considered (Fig. 1). The beam has n cracks located at x_i . The differential equation of free vibration for the

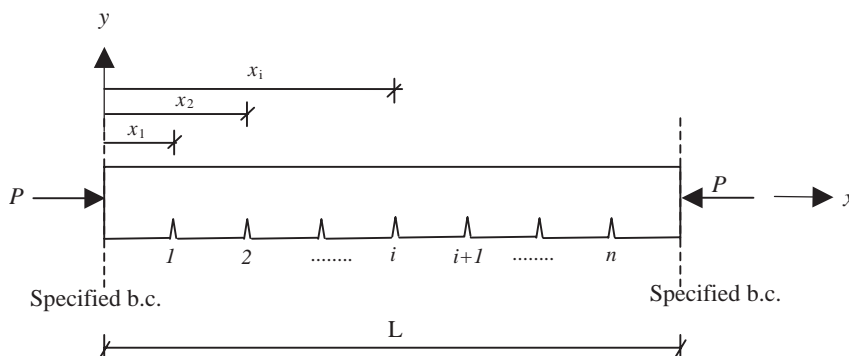


Fig. 1. Beam with n cracks subjected axial force.

uncracked beam assuming constant flexural rigidity and mass density can be written as follows [21]:

$$EI \frac{\partial^4 y}{\partial x^4} + P \frac{\partial^2 y}{\partial x^2} + \rho A \frac{\partial^2 y}{\partial t^2} = 0, \tag{1}$$

where E is the modulus of elasticity, I the moment of inertia of the beam, P the axial load acting on the beam, and ρA are the mass per unit length of the beam. Solution of Eq. (1) with the use of separation of variables is given in the following form:

$$y(x, t) = Y(x)e^{i\omega t}. \tag{2}$$

Substituting Eq. (2) into Eq. (1) yields the differential equation for modal displacements and it is given in the following equation:

$$EI \frac{\partial^4 Y}{\partial x^4} + P \frac{\partial^2 Y}{\partial x^2} - \rho A \omega^2 Y = 0. \tag{3}$$

In Eq. (3), ω is the circular natural frequency of the transverse vibration for the compressed beam. The general solution of Eq. (3) can be written as:

$$Y(x) = C_1 \sinh(\alpha x/L) + C_2 \cosh(\alpha x/L) + C_3 \sin(\beta x/L) + C_4 \cos(\beta x/L) \tag{4}$$

here $C_1, C_2, C_3,$ and C_4 are the constants that need to be evaluated using boundary conditions. α and β are non-dimensional parameters which can be written as:

$$\alpha = \sqrt{-\left(\frac{PL^2}{2EI}\right) + \sqrt{\left(\frac{PL^2}{2EI}\right)^2 + \left(\frac{\rho A}{EI}\right)(\omega L^2)^2}}, \tag{5}$$

$$\beta = \sqrt{\left(\frac{PL^2}{2EI}\right) + \sqrt{\left(\frac{PL^2}{2EI}\right)^2 + \left(\frac{\rho A}{EI}\right)(\omega L^2)^2}}. \tag{6}$$

By setting $\Phi = PL^2/2EI$ and $\Psi = \sqrt{(\rho A/EI)\omega L^2}$, α and β can be expressed as $\alpha = \sqrt{-\Phi + \sqrt{\Phi^2 + \Psi^2}}$, and $\beta = \sqrt{\Phi + \sqrt{\Phi^2 + \Psi^2}}$.

In order to write the general solution (Eq. (4)) as a function of boundary conditions at $x = 0$, Eq. (7) is adopted. This greatly simplifies the solution of the problem and helps to build a systematic approach for the problem considered in this study

$$Y(\chi) = Y(0)A(\chi) + Y'(0)B(\chi) + Y''(0)C(\chi) + Y'''(0)D(\chi). \tag{7}$$

In Eq. (7), χ is the non-dimensional length parameter (x/L), $Y(0)$ is displacement at $\chi = 0$, and other initial parameters $Y'(0), Y''(0),$ and $Y'''(0)$ are related to the boundary conditions such that they give displacement units. These relations are given as $Y'(0) = \theta(0)L, Y''(0) = M(0)L^2/EI, Y'''(0) = Q(0)L^3/EI$ where $\theta(0), M(0), Q(0)$ are the slope, bending moment, and shear at $\chi = 0$, respectively. Functions $A(\chi), B(\chi), C(\chi), D(\chi)$ are appropriately selected linearly independent

non-dimensional functions which satisfy the following condition:

$$\begin{bmatrix} A(0) & A'(0) & A''(0) & A'''(0) \\ B(0) & B'(0) & B''(0) & B'''(0) \\ C(0) & C'(0) & C''(0) & C'''(0) \\ D(0) & D'(0) & D''(0) & D'''(0) \end{bmatrix} = \begin{bmatrix} 1 & 0 & 0 & 0 \\ 0 & 1 & 0 & 0 \\ 0 & 0 & 1 & 0 \\ 0 & 0 & 0 & 1 \end{bmatrix}. \tag{8}$$

It should be noted that Li [8] used a similar identity (Eq. (8)) to describe the modal shape functions of beams in the case of no axial force. In the presence of axial force, functions $A(\chi)$, $B(\chi)$, $C(\chi)$, $D(\chi)$ are given as follows:

$$A(\chi) = H(\chi) + 2\Phi F(\chi), \tag{9}$$

$$B(\chi) = G(\chi) + 2\Phi E(\chi), \tag{10}$$

$$C(\chi) = F(\chi) = \eta[\cosh(\alpha\chi) - \cos(\beta\chi)], \tag{11}$$

$$D(\chi) = E(\chi) = \eta\left[\frac{1}{\alpha} \sinh(\alpha\chi) - \frac{1}{\beta} \sin(\beta\chi)\right], \tag{12}$$

$$G(\chi) = \eta[\alpha \sinh(\alpha\chi) + \beta \sin(\beta\chi)], \tag{13}$$

$$H(\chi) = \eta[\alpha^2 \cosh(\alpha\chi) + \beta^2 \cos(\beta\chi)], \tag{14}$$

where $\eta = 1/(\alpha^2 + \beta^2)$.

For static case (i.e. $\omega = 0$) functions $A(\chi)$, $B(\chi)$, $C(\chi)$, $D(\chi)$ reduce to the equations given below:

$$A(\chi) = 1, \tag{15}$$

$$B(\chi) = \chi, \tag{16}$$

$$C(\chi) = \frac{1}{\beta^2}[1 - \cos(\beta\chi)], \tag{17}$$




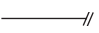
$$D(\chi) = \frac{1}{\beta^2}\left[\chi - \frac{1}{\beta} \sin(\beta\chi)\right]. \tag{18}$$

Using the approach described by Eq. (7), the modal shape functions of the first segment (from the left support to the first crack) of the beam with cracks can be described with the following expression:

$$Y_1(\chi) = Y_1(0)A(\chi) + Y_1'(0)B(\chi) + Y_1''(0)C(\chi) + Y_1'''(0)D(\chi). \tag{19}$$

The boundary conditions at $\chi = 0$, helps reducing Eq. (19) to a form involving only two of the initial parameters. A list of common boundary conditions and the modal shape functions of the

Table 1
Common boundary conditions and mode shape functions of the first segment

Support type	Boundary conditions	Mode shape function of first segment
 (pinned)	$Y(0) = 0$ $Y''(0) = 0$	$Y(\chi) = Y'(0)B(\chi) + Y'''(0)D(\chi)$
 (fixed)	$Y(0) = 0$ $Y'(0) = 0$	$Y(\chi) = Y''(0)C(\chi) + Y'''(0)D(\chi)$
 (guided)	$Y'(0) = 0$ $Y'''(0) = 0$	$Y(\chi) = Y(0)A(\chi) + Y''(0)C(\chi)$
 (free)	$Y''(0) = 0$ $Y'''(0) + 2\Phi Y'(0) = 0$	$Y(\chi) = Y(0)A(\chi) + Y'(0)G(\chi)$

first segment are given in Table 1. A model of massless rotational spring is adopted for the cracks in order to describe the local flexibility due to the presence of cracks [5,6]. According to this representation, continuity of displacement, moment, and shear needs to be satisfied. Furthermore, the jump condition for the slopes at two ends of the crack needs to be satisfied due to the presence of the rotational spring. Based on these arguments following conditions needs to hold at the first crack location:

$$Y_1(\chi_1) = Y_2(\chi_1), \tag{20}$$

$$[Y'_2(\chi_1) - Y'_1(\chi_1)] = C_1 Y''_1(\chi_1), \tag{21}$$

$$Y''_1(\chi_1) = Y''_2(\chi_1), \tag{22}$$

$$Y'''_1(\chi_1) + 2\Phi Y'_1(\chi_1) = Y'''_2(\chi_1) + 2\Phi Y'_2(\chi_1). \tag{23}$$

In Eq. (21), C_1 is the non-dimensional flexibility of the rotational spring representing the effect of crack at first crack location, χ_1 . For a one sided open crack, C_i is given in Eq. (24) [6–8,16,22] as a function of non-dimensional crack severity a_i/h , a_i is the depth of the crack and h is the depth of the section

$$C_i(a_i/h) = 5.346(h/L)(1.8624(a_i/h)^2 - 3.95(a_i/h)^3 + 16.375(a_i/h)^4 - 37.226(a_i/h)^5 + 76.81(a_i/h)^6 - 126.9(a_i/h)^7 + 172(a_i/h)^8 - 143.97(a_i/h)^9 - 66.56(a_i/h)^{10}). \tag{24}$$

The compliance function given Eq. (24) represents the local flexibility introduced due to the presence of a crack. It was derived by Dimarogonas and Paipetis [23] using linear elastic fracture mechanics. Experimental verification of this local flexibility function was presented for cantilever beams with a single crack [22]. Crack positions, and severities (a/h ratios ranging from 0.1 to 0.8) were taken as test variables in the experiments. Closed form expressions to determine eigenvalues of a cantilever beam with a crack were used in their analytical model [22]. Cracks were modeled

using rotational springs with flexibilities given by Eq. (24). Comparisons of analytical results with experimental findings showed that estimated crack locations and severities had errors no larger than 8% and 5%, respectively. These results provide confidence on the accuracy of Eq. (24) which simulates local flexibility due to the presence of a crack. Therefore, further verification of the flexibility function using other numerical analysis tools is not conducted. Instead, details and accuracy of the proposed method are presented below.

In order to satisfy the jump condition of the slopes (Eq. (21)), and continuity of shear at crack locations following expression needs to hold:

$$Y_2(\chi) = Y_1(\chi) + C_1 Y_1''(\chi_1)B(\chi - \chi_1) - 2\Phi C_1 Y_1''(\chi_1)D(\chi - \chi_1). \tag{25}$$

It can be seen that when χ is equal to χ_1 , first derivative of Eq. (25) recovers the jump condition defined by Eq. (21), and third derivative of Eq. (25) recovers the continuity condition defined by Eq. (23). Continuity of displacement and moments are satisfied due to the special character of functions $B(\chi)$, $D(\chi)$ as given per Eq. (8). Generalizing Eq. (25) for the i th crack and making use of Eq. (10) yields the modal shape function for $(i + 1)$ th beam segment:

$$Y_{i+1}(\chi) = Y_i(\chi) + C_i Y_i''(\chi_i)G(\chi - \chi_i). \tag{26}$$

This expression can be used to compute the modal shape function of the $(n + 1)$ th segment as a function of the modal shape function of the first segment. This relationship is given in the following equation:

$$Y_{n+1}(\chi) = Y_1(\chi) + \sum_{i=1}^n C_i Y_i''(\chi_i)G(\chi - \chi_i). \tag{27}$$

$Y_1(\chi)$ is selected from Table 1 depending on the boundary conditions prescribed at $\chi = 0$. As mentioned previously, only two unknowns are involved in this expression. Applying the boundary conditions at the right end of the beam, two equations are obtained with two unknowns. By setting the determinant of this system of two equations equal to zero, eigenfrequencies can be obtained for a beam with multiple cracks located at x_1, x_2, \dots, x_n subjected to an axial load, P . Once the eigenfrequencies are determined, the mode shape functions can easily be determined by relating the two unknowns associated with the boundary conditions at $\chi = 0$ and using Eq. (27). In order to determine the buckling load of the beam containing multiple cracks, a similar procedure can be followed by setting $\omega = 0$ (or $\alpha = 0$).

3. Case studies

3.1. Simply supported beam

First, simply supported beam with a single crack is considered. The boundary conditions at $\chi = 0$ yield the mode shape functions of the first segment in the following form:

$$Y_1(\chi) = Y_1'(0)B(\chi) + Y_1'''(0)D(\chi). \tag{28}$$

Using Eq. (27), the eigenfunction of the second segment is:

$$Y_2(\chi) = Y_1(\chi) + C_1 Y_1''(\chi_1)G(\chi - \chi_1). \tag{29}$$

Substituting Eq. (28) into Eq. (29) and applying the boundary conditions at $\chi = 1$, ($Y_2(1) = 0$, $Y_2''(1) = 0$) following two equations shown in a matrix representation are obtained:

$$\begin{bmatrix} B(1) + C_1 G(1 - \chi_1) B''(\chi_1) & D(1) + C_1 G(1 - \chi_1) D''(\chi_1) \\ B''(1) + C_1 G''(1 - \chi_1) B'(\chi_1) & D''(1) + C_1 G(1 - \chi_1) D''(\chi_1) \end{bmatrix} = \begin{bmatrix} Y_1'(0) \\ Y_1'''(0) \end{bmatrix}. \quad (30)$$

Setting the determinant of the 2×2 matrix given on the left-hand side of Eq. (30), and solving for ω , results in the eigenfrequencies of the cracked beam. For the static case ($\omega = 0$), the characteristic equation can be obtained from the determinant of the same matrix and reduces to the following form:

$$\sin(\beta) - C_1 \beta \sin(\beta \chi_1) \sin(\beta \chi_2) = 0. \quad (31)$$

The analysis presented above is performed in a non-dimensional manner. The parameters that needs to be selected are χ_1 , a_1/h , h/L and P/P_{cr} in order to generate non-dimensional plots for eigenfrequencies. P_{cr} is the Euler buckling load for the simply supported undamaged beam ($P_{cr} = \pi^2 EI/L^2$). In order to determine the non-dimensional buckling load (P/P_{cr}), selection of χ_1 , a_1/h , h/L are sufficient.

Fig. 2 presents the results of analyses for the buckling load of a simply supported beam with a single crack. Non-dimensional crack location χ_1 , are plotted against the non-dimensional buckling load P/P_{cr} for crack severities (a_1/h) ranging from 0.05 to 0.5. This range of crack severities is believed to represent the depth of cracks that occur under service loads. An h/L ratio of 0.1 is selected for all the analyses. Due to symmetry of the beam and the boundary conditions, crack location is varied from the support to the center of the beam. It can be observed that buckling load significantly changes due to the presence of cracks. For a crack with an a_1/h ratio of 0.5

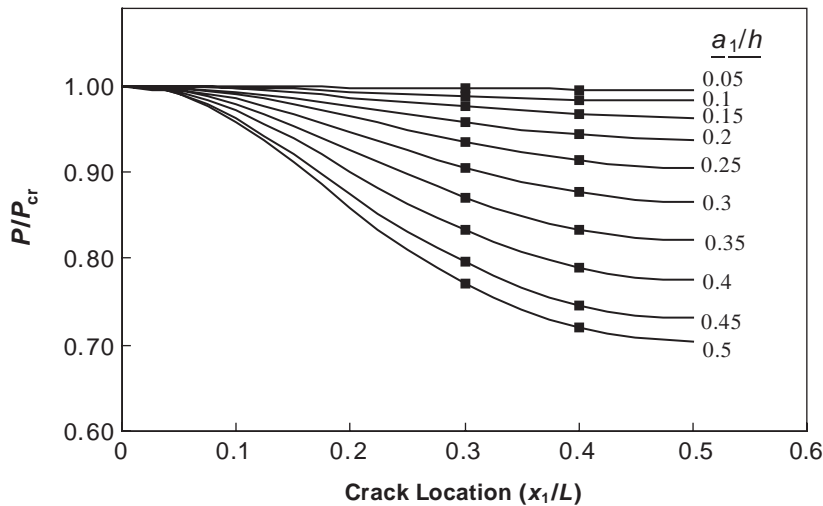


Fig. 2. Buckling loads of the simply supported beam with a single crack located at (x_1/L) for various crack severities (a_1/h values given next to curves); solid lines: analytical solution, dots: finite element analyses.

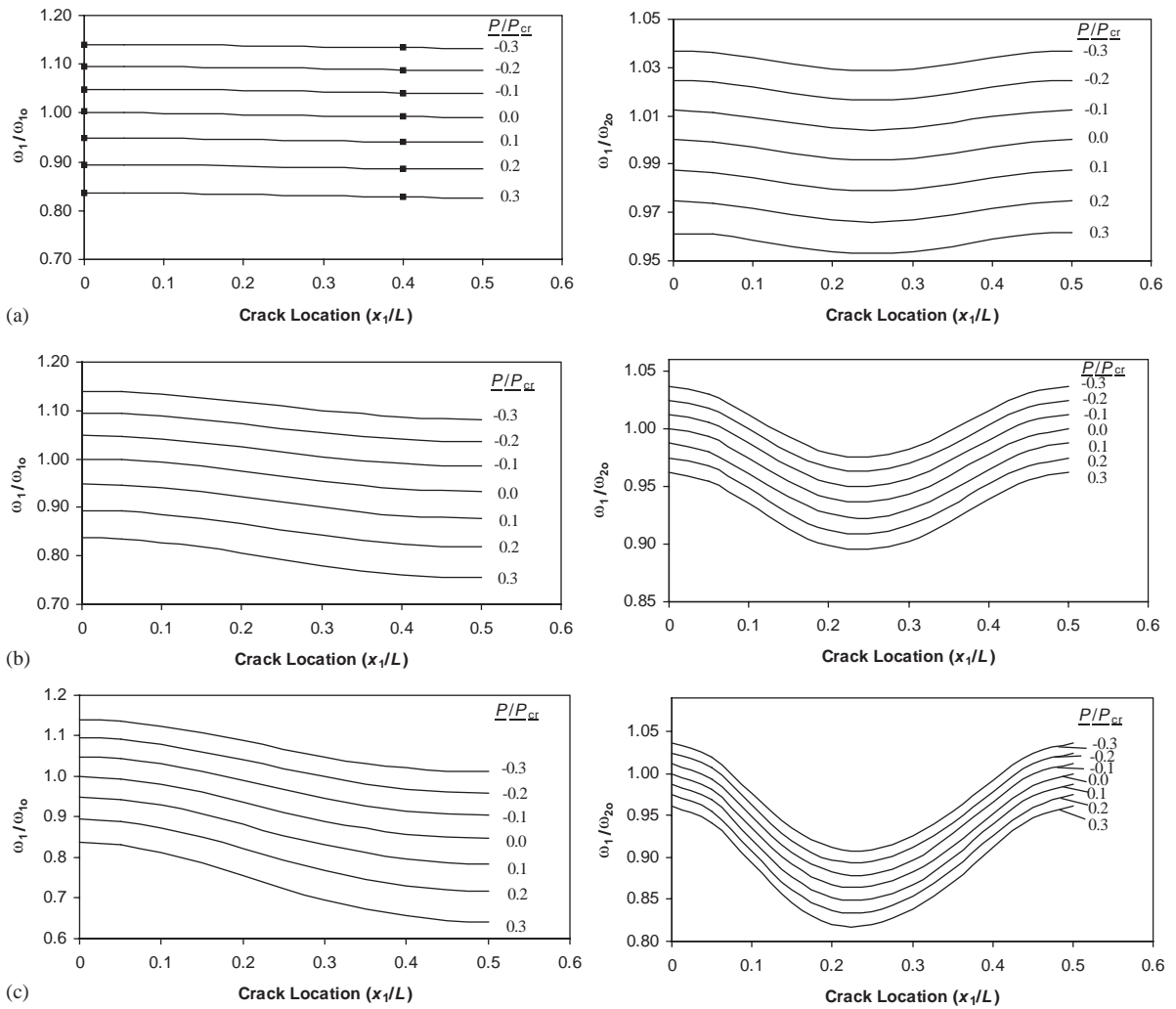


Fig. 3. First and second eigenfrequencies of the simply supported beam with a single crack located at (x_1/L) for different axial loads (P/P_{cr} values given next to curves), and crack severities, (a) $a_1/h = 0.1$, (b) $a_2/h = 0.3$, and (c) $a_1/h = 0.5$; solid lines: analytical solution, dots: finite element analyses.

located at the center of the beam, buckling load decreases about 30%. As expected, deeper cracks closer to the center of the beam result in higher reductions of buckling loads.

Fig. 3 presents the results of eigenfrequencies of the cracked beam divided by the eigenfrequency of the undamaged beam ($\omega_{10} = (\pi/L)^2 \sqrt{EI/\rho A}$, $\omega_{20} = (2\pi/L)^2 \sqrt{EI/\rho A}$). An aspect ratio (h/L) of 0.1 is selected for the analyses and crack location and axial force levels are varied. Three crack severities, and seven axial force levels are used in the analyses. It can be observed that as the crack location approaches to the center of the beam, the reduction in the natural frequency of the beam due to the presence of the crack increases. For the second mode

Table 2
Comparisons of results with finite element analyses for the simply supported beam with two cracks

Parameters					Results from proposed approach			Finite element analyses results		
x_1/L	x_2/L	a_1/h	a_2/h	Axial load (P/P_{cr}^a)	Buckling load (P/P_{cr}^a)	ω_1/ω_{10}^b	ω_2/ω_{20}^c	Buckling load (P/P_{cr}^a)	ω_1/ω_{10}^b	ω_2/ω_{20}^c
0.1	0.4	0.3	0.5	0.1	0.7129	0.7917	0.9223	0.7129	0.7916	0.9221
0.1	0.4	0.3	0.5	0.2		0.7244	0.9085		0.7243	0.9083
0.1	0.4	0.3	0.5	0.3		0.6501	0.8944		0.6500	0.8943
0.1	0.4	0.2	0.4	0.1	0.7850	0.8331	0.9420	0.7851	0.8330	0.9418
0.1	0.4	0.2	0.4	0.2		0.7700	0.9285		0.7699	0.9284
0.1	0.4	0.2	0.4	0.3		0.7012	0.9148		0.7011	0.9147
0.2	0.3	0.3	0.5	0.1	0.7342	0.8105	0.8371	0.7342	0.8104	0.8367
0.2	0.3	0.3	0.5	0.2		0.7442	0.8217		0.7441	0.8214
0.2	0.3	0.3	0.5	0.3		0.6713	0.8060		0.6713	0.8057
0.2	0.3	0.2	0.4	0.1	0.8142	0.8528	0.8773	0.8142	0.8528	0.8771
0.2	0.3	0.2	0.4	0.2		0.7910	0.8627		0.7909	0.8625
0.2	0.3	0.2	0.4	0.3		0.7239	0.8479		0.7238	0.8477

^a $P_{cr} \pi^2 EI/L^2$.
^b $\omega_{10} = (\pi/L)^2 \sqrt{EI/\rho A}$.
^c $\omega_{20} = (2\pi/L)^2 \sqrt{EI/\rho A}$.

frequency, $L/4$ is the location that results in the maximum decrease compared to that of the undamaged beam with axial force. When the axial force is compressive, reductions in the eigenfrequencies are observed whereas increases in eigenfrequencies are observed when the axial force is tensile. It can be observed that even small axial loads, which are actually realistic for service conditions of some structural elements, can result in shifts up to 15% in the first mode eigenfrequencies. This result is important from the point of damage detection using eigenfrequencies. Furthermore, as the crack severity increases (higher a_1/h ratios) reduction in eigenfrequency changes becomes more pronounced.

The results obtained through the use of the proposed method are compared to the results obtained from finite element analyses conducted using ANSYS [24]. The beam is discretized into 50 elements for accurate representation of crack locations, and cracks are modeled using rotational springs whose flexibilities are determined through the use of Eq. (24). In this way, possible modeling errors due to crack representation can be isolated, while verifying the accuracy of the proposed method. The results of finite element analyses are shown in Figs. 2 and 3a. It can be observed that a good agreement is observed between the two solutions, the proposed approach being more efficient once the system of equations is set.

The effect of having the second crack on the buckling loads and eigenfrequency changes are studied next. The problem statement and the second-order determinant to be solved for the simply supported beam with two cracks are given in Appendix A. Cases analyzed using the proposed

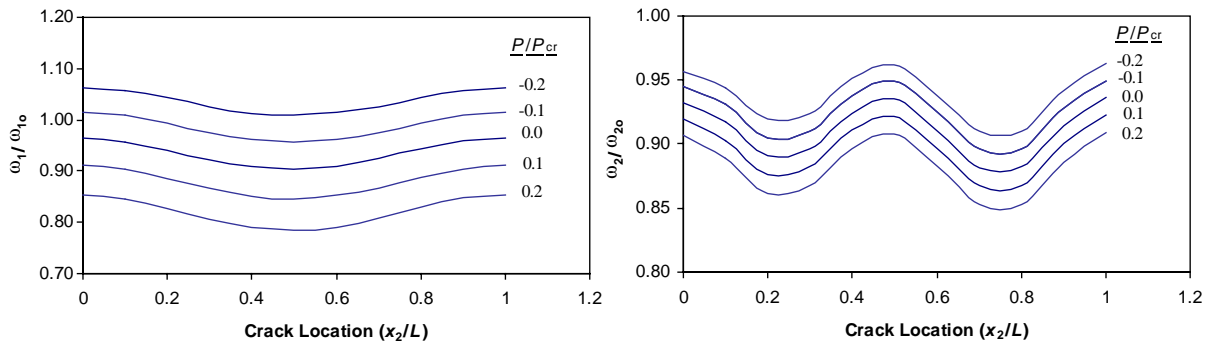


Fig. 4. First and second eigenfrequencies of the simply supported beam with two cracks for different axial loads (P/P_{cr} values given next to curves) and second crack locations (x_2/L); first crack location ($x_1/L = 0.25$), crack severities ($a_1/h = a_2/h = 0.3$).

approach and finite element analyses are given in Table 2. A good agreement between the two solutions is observed both for the buckling loads and eigenfrequencies. It can be observed that eigenfrequency changes due to presence of two cracks are dependent on crack location severity and the applied axial load level. In order to further clarify the effect of the second crack on the eigenfrequencies another set of parametric studies are performed. First crack location (χ_1) is fixed at 0.25, whereas first and second crack severities (a_1/h and a_2/h values) are taken as 0.3. The location of the second crack and axial load levels are varied similar to those presented previously. Results of these analyses are given in Fig. 4. It can be observed that a maximum reduction of about 7% is observed in the first eigenfrequency compared to the case with single crack. In addition, presence of the axial force equal to 20% of the buckling load can change the eigenfrequencies of the damaged beam up to 10%. Another interesting observation is due to the symmetry of the structure. The presence of the second crack at one of the two symmetric locations results in similar changes in eigenfrequencies, resulting in the multiplicity of the solution in the damage identification process.

3.2. Cantilever beam

The analysis of a cantilever beam is performed similar to that presented for the simply supported beam. The approach with the proposed method is presented here for a single crack case, whereas details of the solution for three cracks are presented in Appendix A. The boundary conditions at the free end yield the mode shape functions of the first segment in the following form:

$$Y_1(\chi) = Y_1(0)A(\chi) + Y_1'(0)G(\chi). \tag{32}$$

Using Eq. (27), the eigenfunction of the second segment is:

$$Y_2(\chi) = Y_1(\chi) + C_1 Y_1''(\chi_1)G(\chi - \chi_1). \tag{33}$$

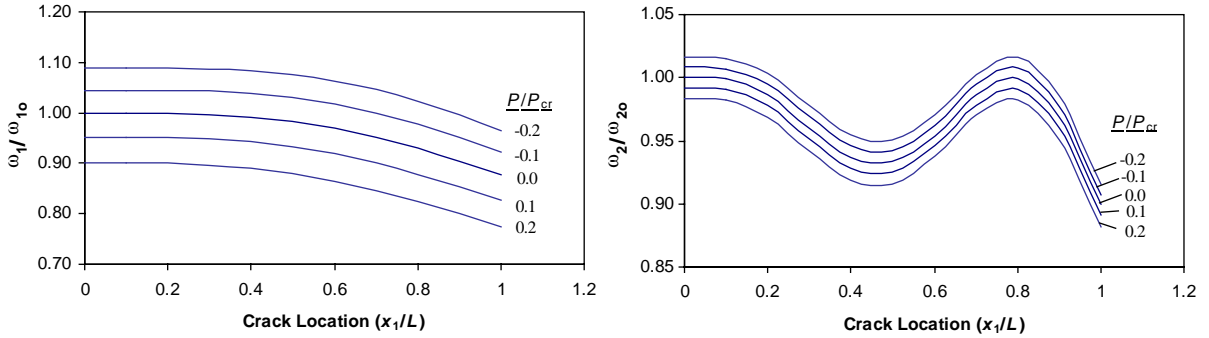


Fig. 5. First and second eigenfrequencies of the cantilever beam with a single crack for different axial loads (P/P_{cr} values given next to curves) and crack locations (x_1/L); crack severity ($a_1/h = 0.3$).

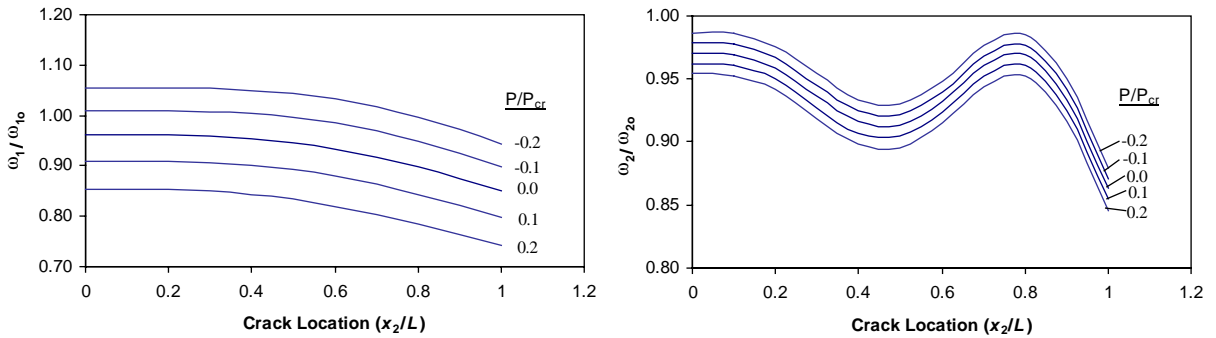


Fig. 6. First and second eigenfrequencies of the cantilever beam with two cracks for different axial loads (P/P_{cr} values given next to curves) and second crack locations (x_2/L); first crack location ($x_1/L = 0.65$), crack severities ($a_1/h = a_2/h = 0.3$).

Substituting Eq. (28) into Eq. (29) and applying the boundary conditions at $\chi = 1$, ($Y_2(1) = 0$, $Y_2'(1) = 0$) following set of equations are obtained:

$$\begin{bmatrix} A(1) + C_1 G(1 - \chi_1) A''(\chi_1) & G(1) + C_1 G(1 - \chi_1) G''(\chi_1) \\ A'(1) + C_1 G'(1 - \chi_1) A''(\chi_1) & G'(1) + C_1 G'(1 - \chi_1) G''(\chi_1) \end{bmatrix} \begin{bmatrix} Y_1(0) \\ Y_1'(0) \end{bmatrix} = 0. \quad (34)$$

Setting the determinant of the matrix given on the left-hand side and solving for ω , gives the eigenfrequencies of the damaged beam for a given level of axial load.

The effect of having a crack ($a_1/h = 0.3$) in a cantilever beam with an aspect ratio of 0.1 is presented in Fig. 5. Non-dimensional frequency parameters are used in these plots where ω_{10} and ω_{20} are the first two eigenfrequencies of the undamaged cantilever beam ($\omega_{10} = (1.875/L)^2 \sqrt{EI/\rho A}$, $\omega_{20} = (4.694/L)^2 \sqrt{EI/\rho A}$ from Ref. [21]). It can be observed that as the crack location approaches to the fixed support, a reduction of about 15% in the first eigenfrequency occurs. An axial load level equal to 20% of the critical buckling load can shift the eigenfrequencies by about 10% compared to the beam with no axial force. It can also be observed

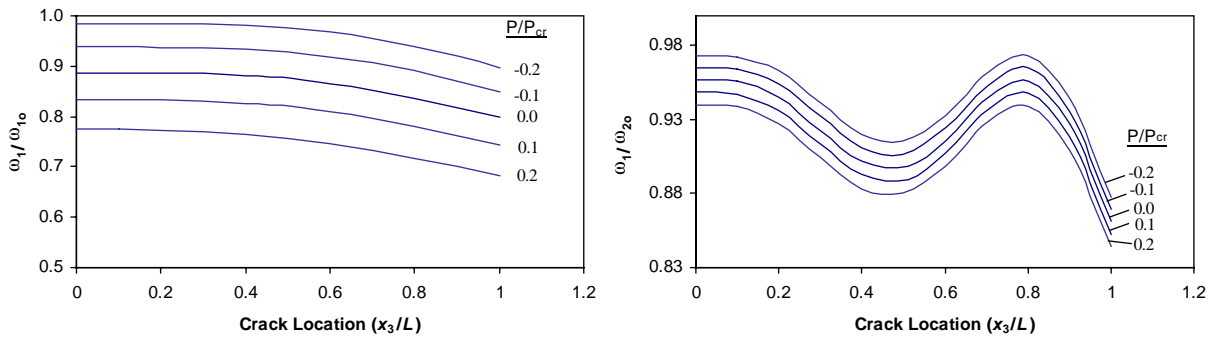


Fig. 7. First and second eigenfrequencies of the cantilever beam with three cracks for different axial loads (P/P_{cr} values given next to curves) and third crack locations (x_3/L); first crack location ($x_1/L = 0.65$), second crack location ($x_1/L = 0.85$), and crack severities ($a_1/h = a_2/h = a_3/h = 0.3$).

that for a crack located within $0.4L$ from the free end; changes in the first eigenfrequencies are minimal compared to that of the undamaged beam with axial force.

The effect of having a second crack is studied by taking the first crack location at $0.65L$ ($\chi_1 = 0.65$) with an a_1/h ratio of 0.3. Second crack severity is assumed to be similar to that of the first crack and its location is varied along the beam length. First and second mode eigenfrequency changes are shown in Fig. 6. The effect of having the second crack on the first eigenfrequency is negligible when the crack is located within $0.4L$ from the free end. However, second mode frequencies change more drastically with the variation of the crack location. It can be observed that there could be multiple second crack locations that would result in the same eigenfrequency changes for the second mode. It can also be stated that axial force tends to affect the first mode eigenfrequencies more than its effect on second mode eigenfrequencies.

Finally, the effect of having a third crack with the crack severity equal to the previous cases is studied. Results presented in Fig. 7 show that similar trends are observed to the case where the effect of second crack is examined. These findings support the fact that axial force magnitudes together with crack locations and severities significantly affect the eigenfrequency changes. In addition, analyses results for three crack cases are compared to the results of the finite element analyses (Table 3). A good agreement between the results of the proposed approach and finite element analyses results are observed. It can also be stated that as the set of three cracks approach to the fixed end significant reductions in the buckling loads can occur (Table 3).

The effect of having intermediate elastic flexible supports on vibration and stability characteristics of beam-columns can also be considered within the context of the proposed approach (Fig. 8). For this purpose, appropriate continuity conditions due to the presence of elastic supports are written and the mode shape function of $(i+1)$ th segment are expressed in terms of the spring constants and mode shape function of i th segment. Then the mode shape functions of the last segment can be determined. Applying appropriate boundary conditions yields a system of equations. Solving for the roots of the second-order determinant gives the

Table 3
Comparisons of results with finite element analyses for the cantilever beam with three cracks

Parameters							Results from proposed approach			Finite element analyses results		
x_1/L	x_2/L	x_3/L	a_1/h	a_2/h	A_3/h	Axial load (P/P_{cr}^a)	Buckling load (P/P_{cr}^a)	ω_1/ω_{10}^b	ω_2/ω_{20}^c	Buckling load (P/P_{cr}^a)	ω_1/ω_{10}^b	ω_2/ω_{20}^c
0.1	0.2	0.3	0.3	0.3	0.3	-0.2	0.9515	1.0862	0.9658	0.9515	1.0860	0.9650
0.1	0.2	0.3	0.3	0.3	0.3	0		0.9967	0.9465		0.9965	0.9457
0.1	0.2	0.3	0.3	0.3	0.3	0.2		0.8947	0.9266		0.8945	0.9259
0.1	0.2	0.3	0.2	0.3	0.5	-0.2	0.9053	1.0838	0.9132	0.9053	1.0836	0.9123
0.1	0.2	0.3	0.2	0.3	0.5	0		0.9922	0.8911		0.9920	0.8903
0.1	0.2	0.3	0.2	0.3	0.5	0.2		0.8867	0.8684		0.8865	0.8675
0.2	0.4	0.6	0.3	0.3	0.3	-0.2	0.8571	1.0579	0.9118	0.8571	1.0578	0.9111
0.2	0.4	0.6	0.3	0.3	0.3	0		0.9620	0.8931		0.9618	0.8924
0.2	0.4	0.6	0.3	0.3	0.3	0.2		0.8511	0.8739		0.8510	0.8732
0.2	0.4	0.6	0.2	0.3	0.5	-0.2	0.7558	1.0229	0.8743	0.7558	1.0227	0.8737
0.2	0.4	0.6	0.2	0.3	0.5	0		0.9189	0.8560		0.9187	0.8553
0.2	0.4	0.6	0.2	0.3	0.5	0.2		0.7966	0.8373		0.7964	0.8366
0.3	0.6	0.9	0.3	0.3	0.3	-0.2	0.7845	0.9776	0.9068	0.7844	0.9775	0.9061
0.3	0.6	0.9	0.3	0.3	0.3	0		0.8803	0.8882		0.8801	0.8876
0.3	0.6	0.9	0.3	0.3	0.3	0.2		0.7669	0.8692		0.7667	0.8686
0.3	0.6	0.9	0.2	0.3	0.5	-0.2	0.6651	0.8814	0.8909	0.6651	0.8862	0.8950
0.3	0.6	0.9	0.2	0.3	0.5	0		0.7787	0.8725		0.7775	0.8767
0.3	0.6	0.9	0.2	0.3	0.5	0.2		0.6564	0.8537		0.6573	0.8581

$$^a P_{cr} = \pi^2 EI / 4L^2.$$

$$^b \omega_{10} = (1.875^2 / L^2) \sqrt{EI / \rho A}.$$

$$^c \omega_{20} = (4.694^2 / L^2) \sqrt{EI / \rho A}.$$

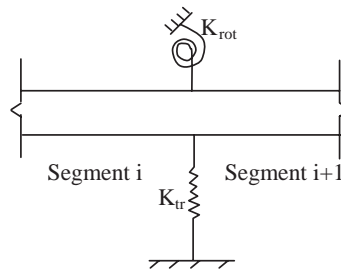


Fig. 8. Intermediate flexible supports.

eigenfrequencies and buckling loads (for the static case) of the beam with multiple cracks and intermediate supports that is subjected to constant axial force. This approach is explained in detail in Appendix B.

4. Conclusions

A new efficient method is proposed to determine eigenfrequency changes of axially loaded beams with multiple cracks. Modal shape functions are written as a function of initial boundary parameters, crack locations and severities. The method is efficient for handling cases with arbitrary number of cracks as the characteristic equation reduces to a second-order determinant. As the static case is approached, buckling load of the beam-column can also be computed. Comparisons of the analytical results with finite element analyses for simply supported and cantilever beams containing up to three cracks have shown good agreement. The method is also extended to include the effect of flexible intermediate supports, which are important for stability and vibration analysis of beam-columns.

The parametric studies conducted on simply supported and cantilever beams showed that eigenfrequency changes due to axial loads are important. Axial loads of about 30% of the critical buckling loads are found to affect first mode eigenfrequencies up to 15%. This effect is observed to be less significant for the second mode eigenfrequencies among the analyzed cases. The presence of open cracks is found to significantly decrease buckling loads depending on the locations and severity of them. In addition, it is shown that crack locations and severities can significantly affect the changes in eigenfrequencies. For the simply supported case, when the first crack location was fixed, different locations of the second crack can result in similar changes in eigenfrequencies leading to the multiplicity of the solution during crack detection process.

The use of the proposed approach is believed to provide an efficient method that can be used in damage identification studies by considering axial loads. It can also serve as a verification method for numerical methods developed for damage detection purposes. Further research is required to experimentally examine the effects of axial force on the changes of eigenfrequencies and buckling loads of cracked beams. In this way, it is possible to show the validity of rotational spring idealization for cracks and open crack assumption adopted in the analyses when axial forces are present.

Appendix A

A.1. Simply supported beam with two cracks

The mode shape functions of the three segments are found as follows:

$$Y_1(\chi) = Y_1'(0)B(\chi) + Y_1'''(0)D(\chi), \quad (\text{A.1})$$

$$Y_2(\chi) = Y_1(\chi) + C_1 Y_1''(\chi_1)G(\chi - \chi_1), \quad (\text{A.2})$$

$$Y_3(\chi) = Y_2(\chi) + C_2 Y_2''(\chi_2)G(\chi - \chi_2). \quad (\text{A.3})$$

Substituting Eqs. (A.1) and (A.2) into Eq. (A.3) and applying the boundary conditions at $\chi = 1$ gives the following system of equations:

$$\begin{bmatrix} K(1) & L(1) \\ K''(1) & L''(1) \end{bmatrix} \begin{bmatrix} Y_1'(0) \\ Y_1'''(0) \end{bmatrix} = 0. \quad (\text{A.4})$$

In which

$$K(\chi) = B(\chi) + C_1 G(\chi - \chi_1)B''(\chi_1) + C_2 G(\chi - \chi_2)[B''(\chi_2) + C_1 G''(\chi_2 - \chi_1)B''(\chi_1)], \quad (\text{A.5})$$

$$L(\chi) = D(\chi) + C_1 G(\chi - \chi_1)D''(\chi_1) + C_2 G(\chi - \chi_2)[D''(\chi_2) + C_1 G''(\chi_2 - \chi_1)D''(\chi_1)]. \quad (\text{A.6})$$

Setting the determinant of the 2×2 matrix given on the left-hand side of Eq. (A.4), and solving for ω , results in the eigenfrequencies of the cracked beam. The relationship between $Y_1'(0)$ and $Y_1'''(0)$ can be obtained from the following equation:

$$Y_1'''(0) = -\frac{K(1)}{L(1)} Y_1'(0). \quad (\text{A.7})$$

Substituting Eq. (A.7) into Eqs. (A.1)–(A.3), mode shape functions of the cracked beam segments can be computed. Appropriate normalizations can be applied to these functions if desired [21].

A.2. Cantilever beam with three cracks

Mode shape functions of segments are determined as follows:

$$Y_1(\chi) = Y_1(0)A(\chi) + Y_1'(0)G(\chi), \quad (\text{A.8})$$

$$Y_2(\chi) = Y_1(\chi) + C_1 Y_1''(\chi_1)G(\chi - \chi_1), \quad (\text{A.9})$$

$$Y_3(\chi) = Y_2(\chi) + C_2 Y_2''(\chi_2)G(\chi - \chi_2), \quad (\text{A.10})$$

$$Y_4(\chi) = Y_3(\chi) + C_3 Y_3''(\chi_3)G(\chi - \chi_3). \quad (\text{A.11})$$

Substituting Eqs. (A.8)–(A.10) into Eq. (A.11), following set of equations is obtained:

$$\begin{bmatrix} M(1) & N(1) \\ M'(1) & N'(1) \end{bmatrix} \begin{bmatrix} Y_1(0) \\ Y_1'(0) \end{bmatrix} = 0, \quad (\text{A.12})$$

where

$$M(\chi) = K(\chi) + C_3 G(\chi - \chi_3) K''(\chi_3), \tag{A.13}$$

$$N(\chi) = L(\chi) + C_3 G(\chi - \chi_3) L''(\chi_3), \tag{A.14}$$

$$K(\chi) = I(\chi) + C_2 G(\chi - \chi_2) I''(\chi_2), \tag{A.15}$$

$$L(\chi) = J(\chi) + C_2 G(\chi - \chi_2) J''(\chi_2), \tag{A.16}$$

$$I(\chi) = A(\chi) + C_1 G(\chi - \chi_1) A''(\chi_1), \tag{A.17}$$

$$J(\chi) = G(\chi) + C_1 G(\chi - \chi_1) G''(\chi_1). \tag{A.18}$$

Setting the determinant of the 2×2 matrix given on the left-hand side of Eq. (A.12), and solving for ω , results in the eigenfrequencies of the cracked beam. The relationship between $Y_1(0)$ and $Y_1'(0)$ can be obtained from the following equation:

$$Y_1'(0) = -\frac{M(1)}{N(1)} Y_1(0). \tag{A.19}$$

The mode shape function of the segments are given below

$$Y_1(\chi) = Y_1(0) \left[A(\chi) - \frac{M(1)}{N(1)} G(\chi) \right], \tag{A.20}$$

$$Y_2(\chi) = Y_1(0) \left[I(\chi) - \frac{M(1)}{N(1)} J(\chi) \right], \tag{A.21}$$

$$Y_3(\chi) = Y_1(0) \left[K(\chi) - \frac{M(1)}{N(1)} L(\chi) \right], \tag{A.22}$$

$$Y_4(\chi) = Y_1(0) \left[M(\chi) - \frac{M(1)}{N(1)} N(\chi) \right]. \tag{A.23}$$

Constant, $Y_1(0)$ is arbitrary and can be determined according to an appropriate normalization [21].

Appendix B

B.1. Intermediate supports

Consider two segments of the beam separated by supports provided by springs (Fig. 8). At the support location, following continuity conditions should be satisfied:

$$Y_i(\chi_s) = Y_{i+1}(\chi_s), \tag{B.1}$$

$$Y_i'(\chi_s) = Y_{i+1}'(\chi_s), \tag{B.2}$$

$$Y''_{i+1}(\chi_s) - Y''_i(\chi_s) = k_{\text{rot}} Y'_i(\chi_s), \quad (\text{B.3})$$

$$Y'''_i(\chi_s) - Y'''_{i+1}(\chi_s) = k_{\text{tr}} Y_i(\chi_s), \quad (\text{B.4})$$

where χ_s is the non-dimensional support location, k_{rot} is the non-dimensional rotational spring constant ($k_{\text{rot}} = K_{\text{rot}}L/EI$ and K_{rot} is the rotational spring stiffness) and k_{tr} is the non-dimensional transverse spring constant ($k_{\text{tr}} = K_{\text{tr}}L^3/EI$ and K_{tr} is the rotational spring stiffness). Eq. (B.5), which expresses the modal shape function of segment $(i+1)$ in terms of modal shape functions of i th segment satisfies these continuity conditions.

$$Y_{i+1}(\chi) = Y_i(\chi) + k_{\text{rot}} Y'_i(\chi_s)C(\chi - \chi_s) - k_{\text{tr}} C_1 Y_1(\chi_s)D(\chi - \chi_s). \quad (\text{B.5})$$

Using this equation the modal shape function of a beam containing n cracks and n_s intermediate supports can be computed using the following expression:

$$Y_{n+1}(\chi) = Y_1(\chi) + \sum_{i=1}^n C_i Y''_i(\chi_i)G(\chi - \chi_i) + \sum_{s=1}^{n_s} k_{\text{rot},s} Y'_s(\chi_s)C(\chi - \chi_s) - \sum_{s=1}^{n_s} k_{\text{tr},s} Y_s(\chi_s)G(\chi - \chi_s). \quad (\text{B.6})$$

Once the mode shape function of the last segment is computed the rest of the solution proceeds similarly as explained in the previous sections. Applying the appropriate boundary conditions at both ends and setting the determinant of the system of equation to zero (similar to Eq. (30)) yields the characteristic equation for the beam with multiple cracks and flexible intermediate supports. Solving for the roots of this equation, the eigenfrequencies of the beam with multiple cracks and intermediate supports subjected to an axial force can be computed.

References

- [1] A.D. Dimarogonas, Vibration of cracked structures: a state of the art review, *Engineering Fracture Mechanics* 55 (5) (1996) 831–857.
- [2] S.W. Doebling, C.R. Farrar, M.B. Prime, Summary review of vibration-based damage identification methods, *Shock and Vibration Digest* 30 (2) (1998) 91–105.
- [3] J. Hu, R.Y. Liang, An integrated approach to detection of cracks using vibration characteristics, *Journal of the Franklin Institute* 330 (5) (1992) 841–853.
- [4] Y. Narkis, Identification of crack location in vibrating simply supported beams, *Journal of Sound and Vibration* 172 (4) (1994) 549–558.
- [5] G.D. Gounaris, C.A. Papadopoulos, A.D. Dimarogonas, Crack identification in beams by coupled response measurement, *Computers and Structures* 58 (2) (1996) 299–305.
- [6] E.I. Shifrin, R. Ruotolo, Natural frequencies of a beam with an arbitrary number of cracks, *Journal of Sound and Vibration* 223 (3) (1999) 409–423.
- [7] Q.S. Li, Vibratory characteristics of multi-step beams with an arbitrary number of cracks and concentrated masses, *Applied Acoustics* 62 (2001) 691–706.
- [8] Q.S. Li, Free vibration analysis of non-uniform beams with an arbitrary number of cracks and concentrated masses, *Journal of Sound and Vibration* 252 (3) (2001) 509–525.
- [9] M. Krawczuk, W.M. Ostachowicz, Transverse natural vibrations of a cracked beam loaded with a constant axial force, *Journal of Vibration and Acoustics, Transactions of the ASME* 115 (4) (1993) 524–528.

- [10] E. Viola, L. Federici, L. Nobie, Detection of crack location using cracked beam element method for structural analysis, *Theoretical and Applied Fracture Mechanics* 36 (2001) 23–35.
- [11] M. Krawczuk, Application of spectral beam finite element with a crack and iterative search technique for damage detection, *Finite Elements in Analysis and Design* 38 (6) (2002) 537–548.
- [12] D.P. Patil, S.K. Maiti, Detection of multiple cracks using frequency measurements, *Engineering Fracture Mechanics* 70 (2003) 553–1572.
- [13] A. Morasi, Crack-induced changes in eigenparameters of beam structures, *ASCE Journal of Engineering Mechanics* 119 (9) (1993) 1798–1803.
- [14] O.S. Salawu, Detection of structural damage through changes in frequency: a review, *Engineering Structures* 19 (9) (1997) 718–723.
- [15] L.W. Chen, C.U. Chen, Vibration and stability of cracked thick rotating blades, *Computers and Structures* 28 (1988) 67–74.
- [16] Q.S. Li, Buckling of multi-step cracked columns with shear deformation, *Engineering Structures* 23 (2001) 356–364.
- [17] S. Naguleswaran, Vibration and stability of an Euler–Bernoulli beam with up to three-step changes in cross-section and axial force, *International Journal of Mechanical Sciences* 45 (2003) 1563–1579.
- [18] I. Takahashi, Vibration and stability of a cracked shaft simultaneously subjected to a follower force with an axial force, *International Journal of Solids and Structures* 35 (23) (1998) 3071–3080.
- [19] K.D. Murphy, A.Y. Zhang, Vibration and stability of a cracked translating beam, *Journal of Sound and Vibration* 237 (2) (2000) 319–335.
- [20] S.P. Timoshenko, G.M. Gere, *Theory of Elastic Stability*, McGraw-Hill, New York, 1961.
- [21] L. Meirovitch, *Elements of Vibration Analysis*, McGraw-Hill, New York, 1975.
- [22] P.F. Rigos, N. Aspragatos, A.D. Dimarogonas, Identification of crack location and magnitude in a cantilever beam from the vibration modes, *Journal of Sound and Vibration* 138 (3) (1990) 381–388.
- [23] A.D. Diamrogonas, S.A. Paipetis, *Analytical Methods in Rotor Dynamics*, Applied Science, London, 1982.
- [24] ANSYS. “ANSYS 6.1 User’s Manual.” Swanson Analysis Systems Inc, 2000.